Tropical Plants

ARTICLE

Open Access

https://doi.org/10.48130/tp-0026-0037

Tropical Plants **2026**, 5: e038

Exploring the systematic positions of two infraspecific taxa of *Dioscorea bulbifera* based on next-generation sequencing technology, morphology and cytology

Authors

Yang-Yang Zhang, Xiao-Qin Sun, Min Chen*, Jia-Yu Xue*

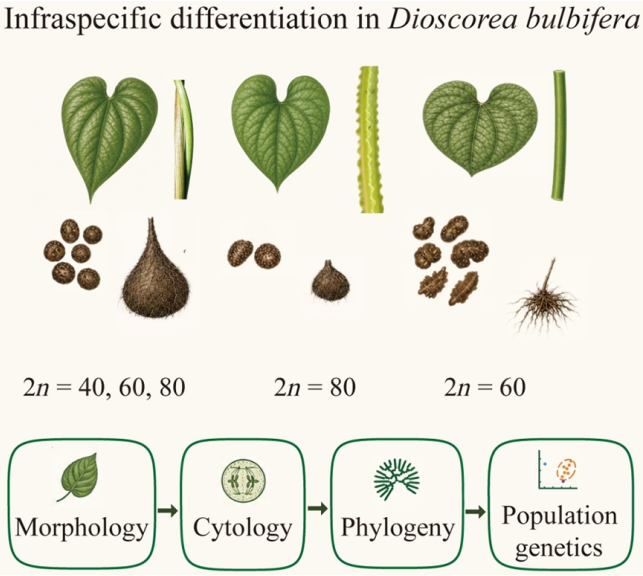
Correspondence

chenmin@cnbg.net (Chen M); xuejy@njau.edu.cn (Xue JY)

In Brief

Integrative morphological, cytological, plastome, and nuclear genomic evidence reveals asymmetric infraspecific differentiation within *Dioscorea bulbifera*. Both *D. bulbifera* f. *domestica* and *D. bulbifera* var. *kacheo* are morphologically diagnosable, but genomic differentiation is stronger in *D. bulbifera* f. *domestica*. The two phylogenies agree on *D. bulbifera* f. *domestica* as an early-diverging lineage, but conflict for *D. bulbifera* var. *kacheo*. Rank comparisons are treated as a working hypothesis, not a formal revision.

Graphical abstract



Highlights

- Morphology distinguishes *D. bulbifera* var. *kacheo* and *D. bulbifera* f. *domestica* from *D. bulbifera* var. *bulbifera*.
- Chromosome counts and flow cytometry corroborate ploidy variation among the sampled accessions.
- Plastome and nuclear trees agree on *D. bulbifera* f. *domestica* but are discordant for *D. bulbifera* var. *kacheo*.
- Genome-wide differentiation is asymmetric and stronger in *D. bulbifera* f. *domestica*.
- Rank comparisons are a working hypothesis pending broader sampling.

Citation: Zhang YY, Sun XQ, Chen M, Xue JY. 2026. Exploring the systematic positions of two infraspecific taxa of *Dioscorea bulbifera* based on next-generation sequencing technology, morphology and cytology. *Tropical Plants* 5: e038 https://doi.org/10.48130/tp-0026-0037

© The Author(s)

Tropical Plants

ARTICLE

Open Access

https://doi.org/10.48130/tp-0026-0037

Tropical Plants **2026**, 5: e038

Exploring the systematic positions of two infraspecific taxa of *Dioscorea bulbifera* based on next-generation sequencing technology, morphology and cytology

Yang-Yang Zhang[1], Xiao-Qin Sun[2,3], Min Chen[2,3*] and Jia-Yu Xue[1*]

[1] *College of Horticulture, Bioinformatics Center, Academy for Advanced Interdisciplinary Studies, Nanjing Agricultural University, Nanjing 210095, China*
[2] *Institute of Botany, Jiangsu Province and Chinese Academy of Sciences, Nanjing 210014, China*
[3] *Jiangsu Key Laboratory for Conservation and Utilization of Plant Resources, Nanjing 210014, China*
* Correspondence: chenmin@cnbg.net (Chen M); xuejy@njau.edu.cn (Xue JY)

Abstract

Dioscorea bulbifera exhibits marked morphological and cytological variation across its wide distribution, underlying long-standing controversy in its infraspecific taxonomy. We combined morphological assessment, cytological analysis, plastome phylogenomics, and genome-wide nuclear single-nucleotide polymorphism data to evaluate the systematic positions of *D. bulbifera* var. *kacheo* and *D. bulbifera* f. *domestica*. Morphology differentiated the taxa in stem architecture, bulbil form, and tuber traits. Among examined accessions, *D. bulbifera* var. *bulbifera* was chromosomally polymorphic ($2n$ = 40, 60, 80), whereas sampled *D. bulbifera* var. *kacheo* ($2n$ = 80) and *D. bulbifera* f. *domestica* ($2n$ = 60) were cytologically uniform at the present sampling scale. Plastome analyses recovered *D. bulbifera* f. *domestica* as a distinct monophyletic lineage, while *D. bulbifera* var. *kacheo* was nested within *D. bulbifera* var. *bulbifera*. Nuclear phylogeny resolved both taxa as well-supported monophyletic groups, revealing cytonuclear discordance. Population genomic analyses showed stronger differentiation of *D. bulbifera* f. *domestica* from *D. bulbifera* var. *bulbifera* than of *D. bulbifera* var. *kacheo*, together with excess allele sharing between *D. bulbifera* var. *kacheo* and *D. bulbifera* f. *domestica*. Thus both entities are morphologically diagnosable, but genomic evidence is asymmetric: *D. bulbifera* f. *domestica* shows stronger genome-wide differentiation consistent with varietal distinctiveness, whereas *D. bulbifera* var. *kacheo* remains only weakly differentiated from *D. bulbifera* var. *bulbifera*. These rank comparisons are treated as a working hypothesis pending broader sampling, not as a formal nomenclatural revision. Integrating morphological, cytological, and genomic evidence is essential for evaluating infraspecific boundaries in ploidy-variable plant groups.

Keywords: Chromosome number, *Dioscorea bulbifera*, Morphological characters, Plastome, Single nucleotide polymorphism (SNP), Phylogenetic analysis

Citation: Zhang YY, Sun XQ, Chen M, Xue JY. 2026. Exploring the systematic positions of two infraspecific taxa of *Dioscorea bulbifera* based on next-generation sequencing technology, morphology and cytology. *Tropical Plants* 5: e038 https://doi.org/10.48130/tp-0026-0037

Introduction

Dioscorea bulbifera is a perennial twining herb in the family Dioscoreaceae[1]. Its tuber, known in traditional Chinese medicine as 'Huangyaozi', has long been used to treat goiter, pharyngitis, pyogenic skin infections, orchitis, and tumors[2,3]. Recent phytochemical and pharmacological reviews have further reported anticancer, anti-inflammatory, antimicrobial, antidiabetic, antioxidant, and immunomodulatory activities of its extracts and bioactive constituents, particularly steroidal saponins, flavonoids, and diterpenoids[2–4]. In addition, the species is cultivated as a food crop in parts of Africa and Asia[2,3] and is grown as an ornamental plant in some regions[5,6]. Morphologically, *D. bulbifera* is characterized by ovoid to pyriform tubers, left-twining stems that are green to purplish, and spherical to ovoid bulbils[1]. Owing to its strong ecological adaptability, *D. bulbifera* is widely distributed across China, Japan, Korea, India, Myanmar, as well as parts of Oceania and Africa[1,2]. This broad geographic range has facilitated the accumulation of substantial intraspecific variation, resulting in considerable morphological diversity[1,2].

The infraspecific taxonomy of *D. bulbifera* has long been controversial. Since the 19th century, multiple taxonomic treatments have been proposed based primarily on morphological grounds, yet no consensus has been reached. Prain & Burkill first provided a synopsis of Old World *Dioscorea*, recognizing *D. bulbifera* var. *kacheo* among other infraspecific taxa[7]; Knuth subsequently recognized eight varieties within *D. bulbifera*[8]; and Prain & Burkill later gave a more detailed account of eastern species, further refining infraspecific delimitation, including *D. bulbifera* var. *heterophylla*[9]. Subsequent studies based on molecular and morphological evidence have continued to refine this framework. Using molecular markers, Zheng et al. reported genetic differentiation between samples from mainland China and those from Hainan and Taiwan[10]. Based on specimen examination and field investigations, Zhou et al. argued for the existence of at least four varieties in China, treating the Hainan entity originally named *D. bulbifera* var. *deltoidea* as *D. bulbifera* var. *heterophylla* Prain & Burkill, and describing var. *brachybotryum* Y.Y. Hang & Y.F. Zhou[11]. These treatments largely document geographically structured morphological variants across the species' wide range[1,11].

Two historically recognized infraspecific taxa are the focus of the present study. *Dioscorea bulbifera* var. *kacheo* Prain & Burkill was first described from the Sikkim Himalaya and adjacent regions to the east[7]. A lectotype for this name was subsequently designated by Hoque et al.[12]. It has been retained in regional treatments such as the *Flora of Bhutan*, where it is diagnosed primarily by stems bearing undulate membranous wings[13]. In contrast, *D. bulbifera* f. *domestica* was originally published as *D. sativa* f. *domestica* Makino[5] and later transferred to *D. bulbifera* f. *domestica*[6]. This taxon has been recognized mainly in Japanese floristic treatments as a

cultivated ornamental form characterized by conspicuous variation in bulbil morphology[6]. These designations follow historical floristic conventions rather than an assessment of evolutionary divergence: in conventional botanical practice, varieties are expected to show geographic, ecological, and/or phylogenetic integrity beyond morphological diagnosability, whereas formae are applied to variants lacking such extramorphological integrity[14]. Nevertheless, most existing classifications of these taxa still rely heavily on morphological traits, which may yield unstable delimitations when environmental effects are not adequately accounted for[11]. In particular, robust integrative evidence supporting the recognition of *D. bulbifera* var. *kacheo* and *D. bulbifera* f. *domestica* remains lacking. Recent low-coverage genome sequencing of Chinese *D. bulbifera* accessions has revealed geographically structured intraspecific lineages based on plastome data[15], yet these analyses did not specifically evaluate the taxonomic status of the two taxa.

Cytological evidence, particularly chromosome number and ploidy level, plays a fundamental role in plant systematics and infraspecific delimitation[16]. Polyploidy is widespread in *Dioscorea*, and the same species frequently comprises multiple cytotypes; diploid, triploid, tetraploid, and higher-ploidy levels have been documented in cultivated yams such as *D. alata* and Guinea yams[17]. For these crops, chromosome counting and flow cytometry provide reliable ploidy estimates[17]. Cross-ploidy hybridization and introgression are also increasingly recognized as important evolutionary processes in plants[18]. For *D. bulbifera*, previous reports likewise indicate marked cytological variation. Asian materials are generally based on $x = 10$, whereas African and American materials have been associated with $x = 9$[16,19]. Somatic chromosome numbers of $2n = 36$, 40, 54, 60, 80, and approximately 100 have been recorded in the literature[16,17,19]. Despite these observations, the relationship between ploidy variation and infraspecific delimitation in *D. bulbifera* has not been explicitly examined. Whether historically recognized varieties and forms differ in chromosome number or ploidy level therefore remains an open question and provides an important line of evidence for clarifying their taxonomic status.

Advances in molecular systematics have provided powerful tools for resolving complex intraspecific relationships in *Dioscorea*. Genome-wide SNP data generated by genotyping-by-sequencing (GBS) or DArTseq, often combined with plastome or phenotypic evidence, have been used successfully to reconstruct population structure, domestication history, and cryptic evolutionary relationships that are difficult to resolve from morphology alone. For example, whole-genome resequencing revealed a hybrid origin of white Guinea yam (*D. rotundata*)[20], and population genomic analyses have clarified domestication and diversification patterns in African yams[21]. SNP- and DArTseq-based studies have likewise resolved genetic structure among cultivated yam accessions, including *D. alata*, *D. rotundata*, and *D. dumetorum*[22]. A high-density genetic map has also been developed for greater yam (*D. alata*)[23]. Plastome phylogenomics has long been a cornerstone of plant maternal lineage reconstruction, and in yams it has proven informative for germplasm discrimination and intraspecific phylogeny[15,24]. For *D. bulbifera* itself, SSR markers, DArTseq SNPs, and plastome data have revealed substantial genetic diversity and geographically structured lineages among accessions from Brazil, West Africa, and China[15,25,26]. However, most of these studies were designed for germplasm characterization or breeding rather than taxonomic delimitation. As a result, the evolutionary relationships and taxonomic status of *D. bulbifera* var. *kacheo* and *D. bulbifera* f. *domestica* remain poorly resolved. Moreover, plastome data alone capture only the maternal genealogy and may be insufficient in groups subject to hybridization or polyploidization[27], whereas nuclear SNP data provide complementary resolution of nuclear genomic history[27]. Integrating morphological, cytological, plastome, and nuclear SNP evidence therefore offers a more robust framework for testing infraspecific boundaries in *D. bulbifera*.

In this study, we employ an integrative approach combining morphological observations, cytological analyses, plastome phylogenomics, and genome-wide nuclear SNP data to address these questions. Specifically, we aim to: (1) assess morphological and cytological differentiation among taxa; (2) reconstruct phylogenetic relationships based on plastome and nuclear genomic data; (3) detect potential gene flow and infer evolutionary processes shaping divergence; and (4) clarify the taxonomic status of *D. bulbifera* var. *kacheo* and *D. bulbifera* f. *domestica*. Our results provide new insights into the evolutionary history of *D. bulbifera* and contribute to a more robust framework for its infraspecific classification.

Materials and methods

Experimental materials

A total of 14 accessions of *D. bulbifera* var. *bulbifera* were collected from different geographic regions across China, including Anhui (AHLA), Fujian (FJNJ), Guangdong (GDSG), Guangxi (GXQZ), Henan (HeNSC), Hunan (HuNXX), Jiangsu (JSYX), Sichuan (SCEM), Zhejiang (ZJLS), Chongqing (CQBB), Yunnan (YNLJ), Hainan (HNHK, HNLS), and Taiwan (TWXB). Accession HNLS was used exclusively for chromosome squashing and flow cytometry. With the exception of HNLS, all remaining accessions, together with two *D. bulbifera* var. *kacheo* accessions (JCHD1, JCHD2) collected from Yunnan Province and two *D. bulbifera* f. *domestica* accessions (YZ1, YZ2) obtained through commercial sources, were subjected to comprehensive analyses (Supplementary Table S1).

Fresh, intact green leaves were collected and immediately preserved by rapid desiccation with silica gel. Voucher specimens corresponding to all accessions were deposited in the Herbarium of the Jiangsu Institute of Botany and the Herbarium of the Chinese Academy of Sciences (NAS) for verification and future reference.

Experimental methods

Ploidy determination by chromosome counting and flow cytometry

Plants of *D. bulbifera* var. *bulbifera*, *D. bulbifera* var. *kacheo*, and *D. bulbifera* f. *domestica* were cultivated in the *Dioscorea* germplasm nursery of Nanjing Zhongshan Botanical Garden (32°3'32.46'' N, 118°49'51.93'' E). Mature bulbils were collected from October to November and stored in sand until April of the following year. After 3–4 weeks of soil cultivation, fresh lateral root tips were collected between 8:00 and 10:00 a.m. during the period of active mitotic division[28]. Root tips were pretreated with 0.002 mol·L^{-1} 8-hydroxyquinoline in the dark for 3 h, fixed in freshly prepared ethanol : glacial acetic acid (3:1) for 24 h at 4 °C (These materials were stored at 4 °C for up to 1–2 weeks before subsequent experiments). After HCl hydrolysis and pectinase treatment, chromosomes were stained with Feulgen's reagent and observed under a microscope at 400×/1,000× magnification[28]. For each accession, chromosome numbers were determined from 5–10 well-spread metaphase cells in which individual chromosomes could be unambiguously distinguished.

Ploidy levels were further estimated by flow cytometry following published protocols for plant DNA flow cytometry[29].

https://doi.org/10.48130/tp-0026-0037

Approximately 20 mg of fresh leaf tissue was placed in a plastic Petri dish and chopped with a sharp razor blade in 1 mL of ice-cold woody plant buffer (WPB: 200 mM Tris-HCl, 4 mM $MgCl_2$, 2 mM Na_2EDTA, 86 mM NaCl, 10 mM sodium metabisulfite, 1% (w/v) PVP, 1% (v/v) Triton X-100, pH 7.5)[30]. The homogenate was mixed gently by pipetting and filtered through a 42 μm nylon mesh into a sample tube. Nuclei were stained with propidium iodide (PI; 50 μg/mL) and treated with RNase (50 μg/mL)[29,30]. Samples were incubated on ice for several minutes to 1 h with occasional shaking before analysis. Relative nuclear DNA content was measured by flow cytometry based on the fluorescence intensity of PI-stained nuclei, and ploidy levels were inferred by comparison with standards of known ploidy.

DNA extraction and next-generation sequencing

Genomic DNA was extracted from approximately 50 mg of silica-gel-dried leaf tissue from each of the 17 samples using the DNAsecure Plant Genome DNA Kit (TIANGEN Biotech, Beijing, China). The purity and integrity of the extracted genomic DNA were assessed by agarose gel electrophoresis and spectrophotometry. The DNA was then fragmented using a Covaris E210 ultrasonicator (Covaris Inc., USA), and fragments sized 200–400 bp were selected using the Agencourt AMPure XP-Medium Kit (Thermo Fisher Scientific, USA). Subsequent steps included end repair, A-tailing, adapter ligation, purification, and PCR amplification to construct Illumina sequencing libraries with an insert size of 150 bp. Library quantification and quality control were performed using Qubit 2.0 and Agilent 2100. The precise concentration of the libraries was determined using q-PCR. Finally, high-throughput sequencing was performed on the Illumina NovaSeq 6000 platform.

Plastome assembly, annotation, and whole plastome sequence comparison

Complete plastomes of *D. bulbifera* were assembled from Illumina paired-end genome skimming data. Raw data were quality-controlled using fastp v0.20.1[31]. Plastomes were assembled *de novo* using GetOrganelle v1.7.6[32] with the parameters: -R 20 -k 21, 51, 91, 121, 131 -F embplant_pt. Plastome sequences of all 17 samples were successfully assembled into complete circular structures. All assembled plastomes were inspected and confirmed to form complete circular molecules with the typical quadripartite structure, including a large single-copy region (LSC), a small single-copy region (SSC), and two inverted repeats (IRs).

The assembled plastomes were annotated using the online software GeSeq[33] (https://chlorobox.mpimp-golm.mpg.de/geseq) by uploading the sequences and selecting *Dioscorea bulbifera* as the reference, generating annotation files and high-resolution circular genome maps. To detect potential expansions or contractions in the inverted repeat (IR) regions within *D. bulbifera* plastomes, a comparison and visualization of the four junctions between the IR and LSC/SSC regions were conducted using IRscope[34] (https://irscope.shinyapps.io/irapp).

Phylogenetic analyses within Dioscorea bulbifera

Phylogenetic analyses were performed using three datasets: (1) complete plastome sequences; (2) concatenated coding sequences (CDS) of 79 protein-coding genes; (3) concatenated amino acid sequences of the same 79 protein-coding genes (Supplementary Table S2), employing *D. nipponica* (OQ525997), *D. alata* (OP787123), and *D. zingiberensis* (NC_027090) as outgroups. All datasets comprised 20 samples, including three *Dioscorea* species as outgroups, and all resulting trees were rooted with *D. zingiberensis*.

Complete plastome sequences were aligned using MAFFT v7[35], and ambiguously aligned regions were removed using trimAl v1.4 with the automated1 option[36]. CDS and amino acid sequences were individually aligned and subsequently concatenated into supermatrices based on gene order and sample IDs. Missing data were treated as gap characters ('–') following standard phylogenomic practice.

Maximum likelihood (ML) phylogenetic analyses were performed using IQ-TREE[37] v3.1.1. The best-fitting substitution models for each dataset were selected using ModelFinder based on the Bayesian Information Criterion (BIC)[38]. Branch support was evaluated using 1,000 ultrafast bootstrap replicates and 1,000 SH-like approximate likelihood ratio test (SH-aLRT) replicates[37]. To reduce potential overestimation of bootstrap support values, the -bnni option was applied, performing additional nearest-neighbor interchange (NNI) optimization during bootstrap analysis[37]. The best-fitting substitution models selected were TVM + F + I for both the plastome and CDS datasets, and Q.BIRD + F + I for the amino acid dataset, as determined by ModelFinder[38].

Bayesian inference (BI) of the complete plastome dataset was conducted in MrBayes v3.2.7[39] under the GTR + I + Γ model, which was used because the BIC-selected TVM + F + I model is unavailable in MrBayes. Two independent MCMC runs with four chains each were run for 1,000,000 generations, sampling every 1,000 generations. Convergence was assessed by an average standard deviation of split frequencies < 0.01 (reported by MrBayes) and by effective sample sizes (ESS) > 200 inspected in Tracer v1.7.2[40]. After discarding the first 25% of sampled trees as burn-in, a majority-rule consensus tree was summarized, and Bayesian posterior probabilities (PP) were calculated. Because ML and BI analyses recovered identical ingroup topologies, and because the CDS and amino acid trees were congruent with the plastome tree, the plastome ML tree is presented with SH-aLRT, UFBoot, and PP support values.

Phylogenetic analysis based on nuclear genome SNPs

Cytological observation revealed ploidy variation among sampled accessions. Because no subgenome-resolved reference genome is available for *D. bulbifera*, sample-specific ploidy was not incorporated into variant calling; instead, genotype likelihoods and SNP matrices were generated under a unified diploid (diploidized) model for all accessions to enable joint cross-accession analyses. Diploidized genotype calling has been applied in autopolyploid GBS studies when sequencing depth was insufficient for reliable tetraploid dosage estimation[41]. Under this diploidized coding, heterozygous states are collapsed into a single heterozygous class, and allelic dosage is not recovered. Comparative analyses indicate that diploidized genotypes can retain analytical utility relative to dosage-aware coding, although some information is lost[42]. Downstream phylogenetic and population-genetic inferences were therefore interpreted primarily in terms of relative placement and differentiation patterns rather than dosage-dependent parameter estimates.

Genome-wide single nucleotide polymorphisms (SNPs) were identified using a standardized Sentieon-based pipeline[43]. The haplotype-resolved genome of *D. bulbifera* var. *bulbifera* (Hainan accession; unpublished) was used as the reference genome. Raw paired-end reads were quality-filtered using fastp v0.23.4[31] with default parameters to remove adapter sequences and low-quality bases. Clean reads were aligned to the reference genome using Sentieon BWA-MEM (Sentieon Genomics, v202308), and alignments were sorted using Sentieon utilities. PCR duplicates were removed using Sentieon Dedup, and alignment statistics, including coverage depth, GC bias, and insert size distribution were calculated using built-in Sentieon modules. Variant calling was performed using Sentieon Haplotyper in GVCF mode (--emit_mode gvcf, --emit_conf

30, --call_conf 30), followed by joint genotyping across all samples to generate a multisample VCF. Outgroup species (*D. nipponica*, *D. alata*, and *D. zingiberensis*) were processed using the same pipeline.

Biallelic SNPs were filtered using GATK-style hard filters (QD < 2.0, MQ < 40.0, FS > 60.0, SOR > 3.0)[44] and PLINK v1.9[45] (--geno 0.15, --maf 0.05). Linkage disequilibrium pruning was performed using PLINK v1.9[45] (--indep-pairwise 50 10 0.2), retaining approximately independent SNPs.

SNP genotypes were converted into a pseudo-sequence alignment in PHYLIP format using TASSEL v5.2.90[46], with heterozygous sites encoded using IUPAC ambiguity codes. Maximum likelihood phylogenetic analysis was conducted using IQ-TREE v3.1.1[37], under the best-fit model (TVM + F + R2) selected by BIC, with branch support assessed using 1,000 ultrafast bootstrap replicates (-bnni).

Population genetic analysis based on nuclear genome SNPs

The 17 in-group samples were assigned to three populations: HD (*D. bulbifera* var. *bulbifera*), JC (*D. bulbifera* var. *kacheo*), and YZ (*D. bulbifera* f. *domestica*). Nucleotide diversity (π) and genetic differentiation (F_{ST}) were calculated using VCFtools v0.1.16[47].

Gene flow was assessed using the *D*-statistic (ABBA–BABA test) implemented in Dsuite v0.4[48], with the topology (HD, JC, YZ, O), where O represents the outgroup. Statistical significance was evaluated using block jackknife resampling.

For demographic inference, LD pruning was performed using PLINK (--indep-pairwise 50 10 0.1). TreeMix v1.13[49] was used to infer population splits and migration events, with the outgroup specified as the root. Migration edges (m = 0–5) were tested with 10 independent runs per model. The optimal number of migration events was determined using OptM[50].

Population structure was analyzed using LD-pruned SNPs. Principal component analysis (PCA) was performed using PLINK v1.9[45] (--pca). ADMIXTURE v1.3.0[51] was run for K = 1–8 with cross-validation (--cv), and the optimal K was selected based on the lowest cross-validation error.

Results

Comparison of morphological traits

The female inflorescences of the three taxa were essentially uniform in morphology (Fig. 1a–c). They are spicate, solitary or several together in the leaf axils, pendulous, with sessile florets closely adpressed to the rachis; the florets bear six white tepals and six staminodes (Fig. 1d–f). This uniformity indicates that the structure of reproductive organs is relatively conservative at the intraspecific level, whereas the principal differences among the three taxa lie in the vegetative organs, as detailed below.

Leaf morphology (Fig. 1g–i) shows moderate variation. Both *D. bulbifera* var. *bulbifera* and *D. bulbifera* var. *kacheo* exhibited broadly ovate-cordate leaves, whereas *D. bulbifera* f. *domestica* showed broadly cordate leaves with a length nearly equal to the width.

Stem morphology (Fig. 1j–l) exhibited more pronounced differentiation. *Dioscorea bulbifera* var. *kacheo* was characterized by ridged stems with membranous wings along the ridges, a feature absent in the other taxa. In contrast, both *D. bulbifera* var. *bulbifera* and *D. bulbifera* f. *domestica* possessed terete stems, sometimes with longitudinal striations. The stems of *D. bulbifera* var. *bulbifera* are often dark red or green with red stripes, while the stems of *D. bulbifera* f. *domestica* are usually emerald green and subglabrous.

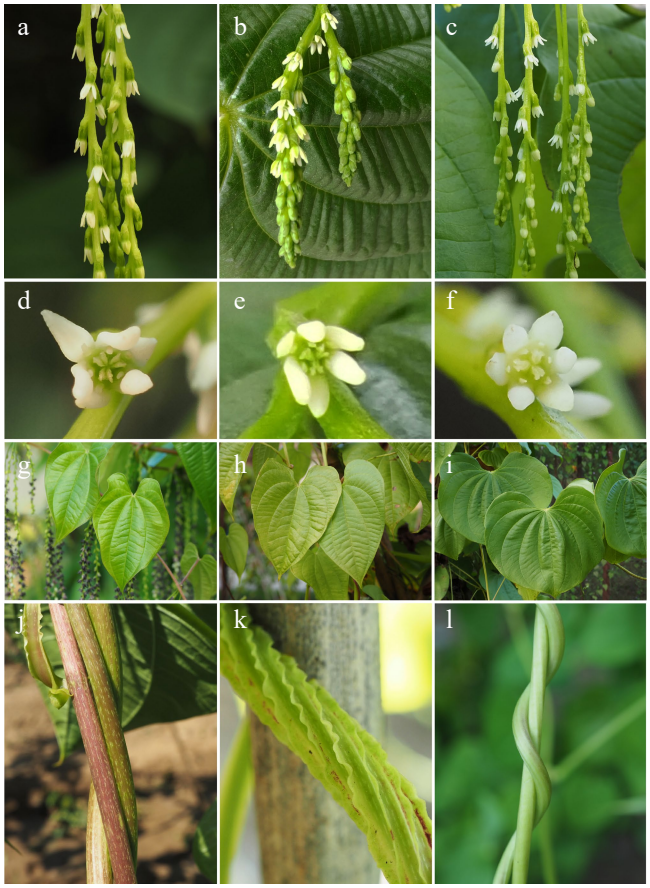


Fig. 1 (a), (d), (g), (j) Morphological comparison of *D. bulbifera* var. *bulbifera*; (b), (e), (h), (k) *D. bulbifera* var. *kacheo*; and (c), (f), (i), (l) *D. bulbifera* f. *domestica*. (a)–(c) Female inflorescences; (d)–(f) female flowers; (g)–(i) leaves; (j)–(l) stems.

Bulbil morphology (Fig. 2a–c) varied substantially among taxa. *Dioscorea bulbifera* var. *bulbifera* produced subglobose bulbils with irregularly arranged depressions, whereas *D. bulbifera* var. *kacheo* bore subglobose to broadly ellipsoid bulbils with regularly arranged protuberances. In contrast, *D. bulbifera* f. *domestica* exhibited highly variable bulbil morphology, often ridged and bearing irregularly arranged protuberances of different sizes.

Tuber morphology (Fig. 2d–f) differed conspicuously among the three taxa. *Dioscorea bulbifera* var. *bulbifera* formed well-developed, swollen underground tubers that occasionally reach several kg in weight. These tubers are usually subglobose to ovoid-globose, with a blackish-brown and easily detached epidermis and yellow flesh, and they give rise to several adventitious roots. The tubers of *D. bulbifera* var. *kacheo* are essentially similar in morphology and structure to those of *D. bulbifera* var. *bulbifera*, differing mainly in their somewhat smaller size (4.0–5.0 vs 8.0–13.0 cm in diameter). In marked contrast, *D. bulbifera* f. *domestica* scarcely forms tubers (1.0–1.5 cm in diameter where present); instead, the junction between the stem and rhizome bears well-developed adventitious roots. Quantitative measurements of tuber diameter for the three taxa are provided in Table 1.

Chromosome number and genome size estimates

Chromosomes were extremely small and dot-like across all samples, requiring well-spread metaphase plates for accurate counting

https://doi.org/10.48130/tp-0026-0037

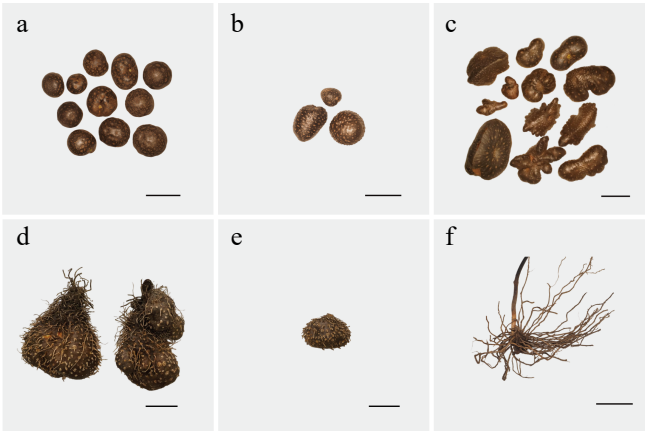


Fig. 2 Morphological comparison of (a), (d) *D. bulbifera* var. *bulbifera*; (b), (e) *D. bulbifera* var. *kacheo*; and (c), (f) *D. bulbifera* f. *domestica*. (a)–(c) Bulbils. (d)–(f) Tubers. Scale bar = 5 cm.

(Fig. 3). In *D. bulbifera* var. *bulbifera*, chromosome numbers varied among the examined accessions: the Hainan Lingshui accession (HNLS) had $2n = 40$ (Fig. 3a), the Hainan Haikou accession (HNHK) had $2n = 60$ (Fig. 3b), and the Zhejiang Lishui accession (ZJLS) had $2n = 80$ (Fig. 3c). In contrast, the examined accession of *D. bulbifera* var. *kacheo* (JCHD1) consistently showed $2n = 80$ across all counted cells (Fig. 3d), and *D. bulbifera* f. *domestica* (YZ1) uniformly displayed $2n = 60$ (Fig. 3e).

To further corroborate these ploidy differences, genome sizes of representative accessions of the three taxa were estimated by flow cytometry (Table 2). The two $2n = 80$ accessions (ZJLS, 1.31 Gb; JCHD1, 1.38 Gb) had the largest genome sizes, approximately twice that of the $2n = 40$ accession (HNLS, 0.66 Gb), whereas the two $2n = 60$ accessions (HNHK, 1.02 Gb; YZ1, 1.15 Gb) showed intermediate values, with minor variation among accessions sharing the same chromosome number. Thus, the proportional differences in genome size among accessions are consistent with the ratios of their chromosome numbers.

Plastome features and comparison

A total of 17 plastomes were assembled (Supplementary Table S2; Fig. 4), with genome sizes ranging from 152,970 to 153,256 bp. The smallest genome was observed in the *D. bulbifera* var. *bulbifera* accession HeNSC (152,970 bp), whereas the largest genome was found in *D. bulbifera* f. *domestica* accession YZ2 (153,256 bp).

All plastomes exhibited the typical quadripartite structure, comprising a pair of inverted repeats (IRs: 25,499–25,505 bp), a large single-copy (LSC: 83,120–83,394 bp), and a small single-copy (SSC: 18,851–18,855 bp) region (Supplementary Fig. S1). The overall GC content was identical across all samples (37.0%), regardless of geographic origin or taxonomic grouping (Supplementary Table S2). Each plastome contained 113 genes, including 79 protein-coding genes, 30 tRNA genes, and 4 rRNA genes, with 19 genes duplicated in the IR regions. Gene content and order were highly conserved across all accessions.

Comparative analysis of IR/SC junctions revealed highly consistent boundary configurations among all samples (Supplementary Fig. S1). Specifically, the LSC/IRb boundary (JLB) was located within the *rps19* gene, while the LSC/IRa boundary (JLA) was positioned in the *psbA-trnH* intergenic region. The SSC/IRb boundary (JSB) occurred within the *ycf1* gene, and the SSC/IRa boundary (JSA) was located adjacent to *ndhF*. Only minor length variation (≤ 6 bp) in IR regions was detected in two *D. bulbifera* f. *domestica* accessions (YZ1 and YZ2), without altering the overall boundary structure.

Phylogenetic relationships, population structure, and gene flow

We first inferred maximum-likelihood (ML) trees from the concatenated coding sequences (CDS) and amino acid sequences of 79 plastid genes (Supplementary Figs. S2, S3). In both trees, only the monophyly of *D. bulbifera* f. *domestica* received strong support, whereas relationships among the remaining ingroup accessions were poorly resolved. We therefore analysed the complete plastome alignment using both ML and Bayesian inference (BI). These whole-plastome analyses provided stronger resolution of infraspecific relationships within *D. bulbifera*. Because ML and BI recovered identical ingroup topologies, only the ML tree is presented (Fig. 5a), with SH-aLRT, UFBoot, and PP values annotated on the nodes.

In the plastome phylogeny (Fig. 5a), the two *D. bulbifera* f. *domestica* accessions formed a strongly supported monophyletic clade that was recovered as sister to all remaining *D. bulbifera* samples (SH-aLRT/UFBoot/PP = 100/100/1.00). *Dioscorea bulbifera* f. *domestica* therefore constitutes an early-diverging lineage within the species. By contrast, the two *D. bulbifera* var. *kacheo* accessions failed to cluster into a single clade. Instead, they were recovered as a monophyletic clade together with *D. bulbifera* var. *bulbifera* populations from southeastern, southern, and southwestern China (Fujian, Taiwan, Guangdong, Guangxi, Chongqing) (SH-aLRT/UFBoot/PP = 100/100/1.00).

In the nuclear SNP phylogeny (Fig. 5b), *D. bulbifera* f. *domestica* also formed a distinct, well-supported clade (SH-aLRT/UFBoot = 100/100) that was sister to the remaining ingroup. *Dioscorea bulbifera* var. *kacheo*, however, was no longer nested within *D. bulbifera* var. *bulbifera*: JCHD1 and JCHD2 formed a strongly supported clade (SH-aLRT/UFBoot = 100/100), which was sister to a clade comprising

Table 1. Morphological traits of three taxa in *Dioscorea bulbifera*.

Organ	Character	*D. bulbifera* var. *bulbifera*	*D. bulbifera* var. *kacheo*	*D. bulbifera* f. *domestica*
Leaf	Shape	Broadly ovate-cordate or ovate-cordate	Broadly ovate-cordate or ovate-cordate	Broadly cordate, length nearly equal to width
	Length/width ratio	1.20–1.60	1.17–1.38	1.02–1.07
Stem	Shape	Terete	Ridged	Terete
	Epidermal color	Often dark red, or green with red stripes	Pale green	Usually emerald green
	Epidermal features	Longitudinally striate	With membranous wings along the ridges	Subglabrous, sometimes longitudinally striate
Bulbil	Shape	Subglobose	Subglobose to broadly ellipsoid	Highly variable in shape, ridged
	Epidermal features	Irregularly arranged depressions	Regularly arranged protuberances	Irregularly arranged protuberances of various sizes
	Diameter (cm)	2.9–4.7	2.8–6.5	2.0–8.5
Tuber	Diameter (cm)	8.0–13.0	4.0–5.0	1.0–1.5

Data were collected from mature field specimens ($n \geq 5$ per taxon). Diameters of bulbils and tubers were measured at the widest transverse position.

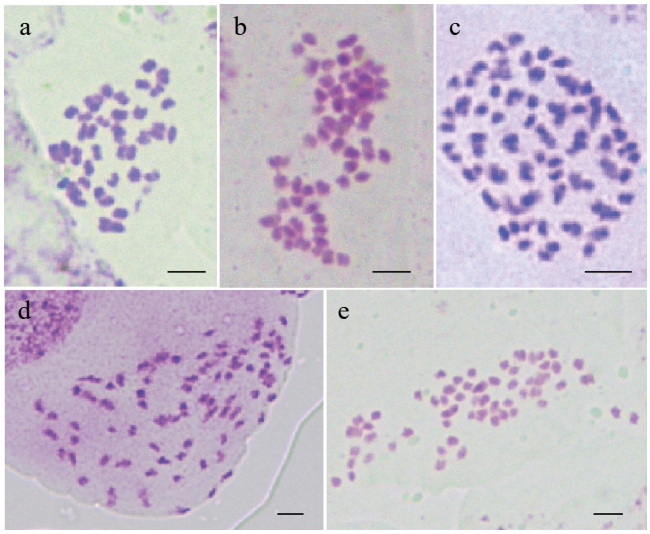


Fig. 3 Chromosome spreads of *D. bulbifera* var. *bulbifera*, *D. bulbifera* var. *kacheo* and *D. bulbifera* f. *domestica*. (a) *D. bulbifera* var. *bulbifera* (HNLS, 2*n* = 40); (b) *D. bulbifera* var. *bulbifera* (HNHK, 2*n* = 60); (c) *D. bulbifera* var. *bulbifera* (ZJLS, 2*n* = 80); (d) *D. bulbifera* var. *kacheo* (JCHD1, 2*n* = 80); (e) *D. bulbifera* f. *domestica* (YZ1, 2*n* = 60). Scale bar = 2 μm.

all *D. bulbifera* var. *bulbifera* accessions (SH-aLRT/UFBoot = 100/100). *Dioscorea bulbifera* var. *bulbifera* itself was likewise recovered as a single well-supported clade (SH-aLRT/UFBoot = 100/100).

Thus, the two trees are concordant in placing *D. bulbifera* f. *domestica* as a distinct early-diverging lineage, but they are discordant for *D. bulbifera* var. *kacheo*: this taxon is nested within *D. bulbifera* var. *bulbifera* in the plastome tree, yet recovered as an independent sister clade to *D. bulbifera* var. *bulbifera* in the nuclear SNP tree (Fig. 5).

PCA and ADMIXTURE analyses were used to further resolve population structure. PCA separated the three groups, with PC1 (16.91%) and PC2 (13.39%) explaining 30.30% of the total genetic variation (Fig. 6a). *Dioscorea bulbifera* f. *domestica* formed a distinct cluster completely separated from *D. bulbifera* var. *bulbifera* and *D. bulbifera* var. *kacheo*, whereas *D. bulbifera* var. *kacheo* was positioned at the periphery of the HD cluster.

ADMIXTURE analysis showed that $K = 1$ had the lowest cross-validation error (Supplementary Fig. S4). At $K = 2$, *D. bulbifera* f. *domestica* was differentiated from the *D. bulbifera* var. *bulbifera*/*D. bulbifera* var. *kacheo* groups with minimal admixture (Fig. 6b); this model was retained for its stronger biological interpretability.

Nucleotide diversity and genetic differentiation were consistent with these patterns (Fig. 6c). JC exhibited the highest nucleotide diversity ($\pi = 6.380 \times 10^{-3}$), followed by *D. bulbifera* var. *bulbifera* and *D. bulbifera* f. *domestica*. Pairwise F_{ST} values indicated strong differentiation between JC and *D. bulbifera* f. *domestica* (0.5051), intermediate differentiation between *D. bulbifera* var. *bulbifera* and *D. bulbifera* f. *domestica* (0.2801), and the lowest between *D. bulbifera* var. *bulbifera* and *D. bulbifera* var. *kacheo* (0.0752).

D-statistic analyses (Supplementary Fig. S5) yielded significantly positive values (D[HD, JC, YZ, O] > 0, $|Z| > 3$, $p < 0.001$), indicating excess allele sharing between *D. bulbifera* var. *kacheo* and *D. bulbifera* f. *domestica*. TreeMix analysis identified $m = 1$ as the optimal model by the Δm method and revealed a single migration edge from YZ to JC (weight = 0.183) (Fig. 6d; Supplementary Figs. S6, S7).

Collectively, these results show that *D. bulbifera* var. *bulbifera* and *D. bulbifera* var. *kacheo* are genetically closely related and only weakly differentiated, whereas *D. bulbifera* f. *domestica* is clearly separated from both groups. Significant *D*-statistic and TreeMix signals of excess allele sharing between *D. bulbifera* var. *kacheo* and *D. bulbifera* f. *domestica* were also detected.

Discussion

Infraspecific differentiation and taxonomic implications in *Dioscorea bulbifera*

Our integrative dataset revealed clear morphological and cytological differentiation among the three taxa, together with pronounced asymmetry in their levels of genomic divergence. Morphologically, both focal taxa are readily diagnosable against *D. bulbifera* var. *bulbifera*: *D. bulbifera* var. *kacheo* is characterized by ridged stems bearing membranous wings along the ridges, whereas *D. bulbifera* f. *domestica* is distinguished by broadly cordate leaves with length nearly equal to width, highly variable and often ridged bulbils, and the near absence of swollen underground tubers. Cytologically, chromosome counts and concordant flow-cytometric genome-size estimates revealed ploidy variation within *D. bulbifera*: the examined *D. bulbifera* var. *bulbifera* accessions spanned 2*n* = 40, 60, and 80, whereas the sampled accessions of *D. bulbifera* var. *kacheo* (2*n* = 80) and *D. bulbifera* f. *domestica* (2*n* = 60) were each uniform and differed from one another, indicating that cytotype variation is partitioned among as well as within infraspecific taxa.

Phylogenomic and population-genetic analyses further resolved the two taxa, but to markedly different degrees. *Dioscorea bulbifera* f. *domestica* was consistently differentiated by every class of molecular evidence: it formed a strongly supported, early-diverging lineage in the plastome tree, a maximally supported clade in the nuclear SNP tree, and a discrete cluster in PCA, carried a nearly undiluted ancestry component in ADMIXTURE, and showed substantial differentiation from *D. bulbifera* var. *bulbifera* ($F_{ST} = 0.2801$). In contrast, *D. bulbifera* var. *kacheo* was not separable from *D. bulbifera* var. *bulbifera* in several analyses: it was nested among *D. bulbifera* var. *bulbifera* accessions in the plastome tree, occupied the periphery of the

Table 2. Estimated genome size of *Dioscorea bulbifera* accessions determined by flow cytometry.

	Sample name	Internal reference	Reference fluorescence intensity	Target fluorescence intensity	Ratio	Estimated genome size (Gb)
D. bulbifera var. *bulbifera*	ZJLS	*Zea mays*	105.51	60.01	0.57	1.31
	HNHK	*Zea mays*	44.22	19.62	0.44	1.02
	HNLS	*Zea mays*	50.97	14.69	0.29	0.66
D. bulbifera var. *kacheo*	JCHD1	*Solanum lycopersicum*	22.58	35.53	1.57	1.38
D. bulbifera f. *domestica*	YZ1	*Zea mays*	44.46	22.14	0.5	1.15

https://doi.org/10.48130/tp-0026-0037

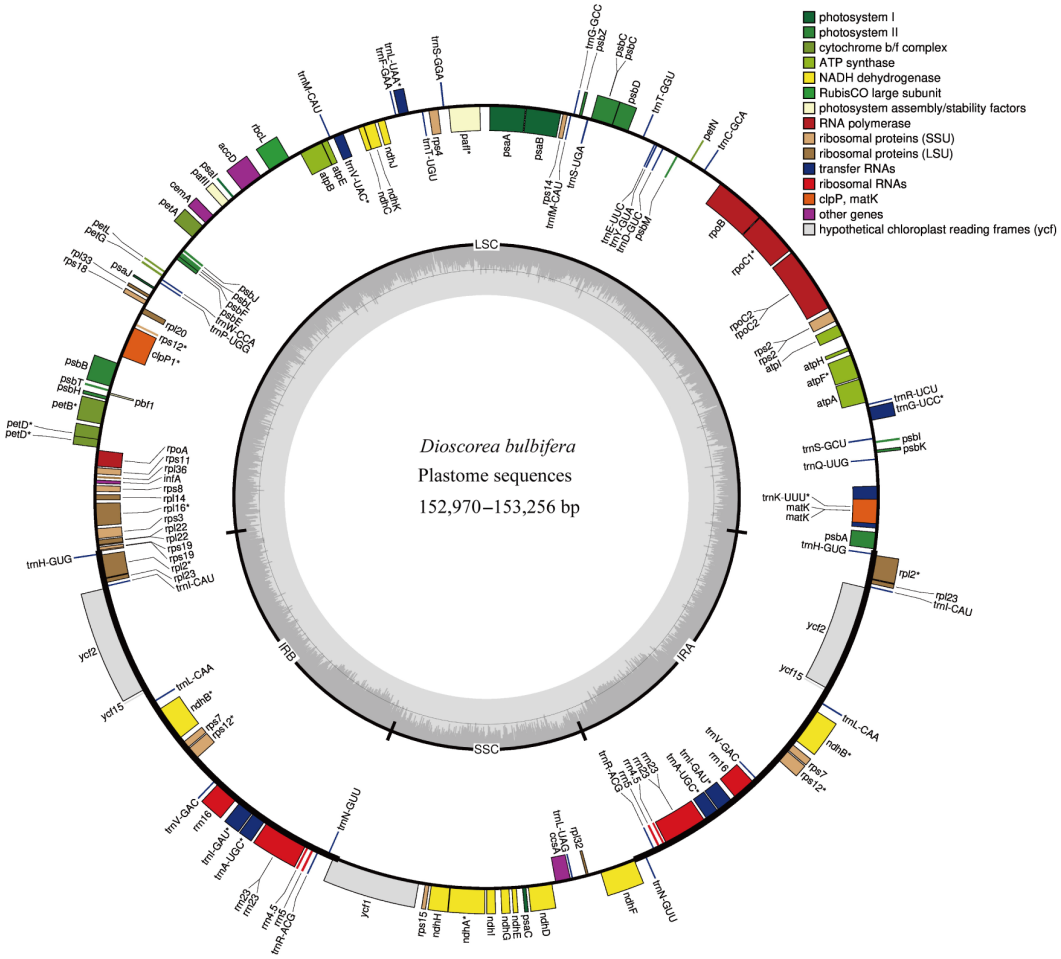


Fig. 4 Plastome map of *D. bulbifera*. Genes on the outer circle are transcribed clockwise, and those on the inner circle are transcribed counterclockwise. Functional categories are indicated by color-coded genes. The dark grey and the light grey plots in the inner circle correspond to the GC content and AT content, respectively.

var. bulbifera cluster in PCA, and showed only weak genome-wide differentiation (F_{ST} = 0.0752), although it was recovered as a distinct clade in the nuclear SNP tree. Concordance among independent character systems is widely used to evaluate lineage separation[52], and integrative morphological–genomic frameworks have proven effective for refining taxon boundaries in angiosperms, including *Dioscorea*[53]. On this basis, *D. bulbifera* f. *domestica* more closely approximates a genetically differentiated infraspecific lineage than does *D. bulbifera* var. *kacheo*.

The *D. bulbifera* var. *kacheo* pattern—clear morphological diagnosis without commensurate genome-wide differentiation from *D. bulbifera* var. *bulbifera*—indicates incongruence between phenotype and nuclear population structure. Pronounced phenotypic differentiation accompanied by weak genetic isolation has been reported in *Dianthus virgineus*[54], and incongruence between phenotypic clusters and genomic lineages has likewise been documented in the *Aquilegia viridiflora* complex[55]. Morphological diagnosability alone is therefore insufficient to equate *D. bulbifera* var. *kacheo* with *D. bulbifera* f. *domestica* in degree of evolutionary independence.

This asymmetry is at odds with historical floristic treatments that assigned varietal rank to *D. bulbifera* var. *kacheo* and forma rank to *D. bulbifera* f. *domestica*; those assignments reflect regional morphological conventions rather than relative levels of genome-wide differentiation. In botanical practice, varieties are generally circumscribed as morphologically diagnosable entities that additionally possess geographic, ecological, and/or phylogenetic integrity, whereas formae are applied to morphological variants lacking such extramorphological integrity[14]. Following this conventional distinction, and integrative approaches emphasizing cross-validation among evidence classes[52,53], we applied operational criteria under which varietal status requires simultaneous support from diagnosable morphology, substantial genome-wide differentiation, and concordance across phylogenomic and population-genetic analyses; morphological divergence without accompanying genome-wide differentiation is regarded as more consistent with forma[54,55]. Under these criteria, *D. bulbifera* f. *domestica* more closely meets the evidentiary expectations of varietal rank, whereas *D. bulbifera* var. *kacheo* satisfies the morphological criterion primarily. Given that each focal taxon was represented by only two accessions from narrow ranges, and that the observed cytological uniformity may not hold across their full distributions, formal nomenclatural rearrangement would be premature. We therefore retain the historically applied ranks and treat the ranking implied by our data as a testable working hypothesis; expanded sampling of *D. bulbifera* var. *kacheo* in Bhutan and adjacent regions and of wild *D. bulbifera* f. *domestica* populations in Japan will be required before formal revision can be justified.

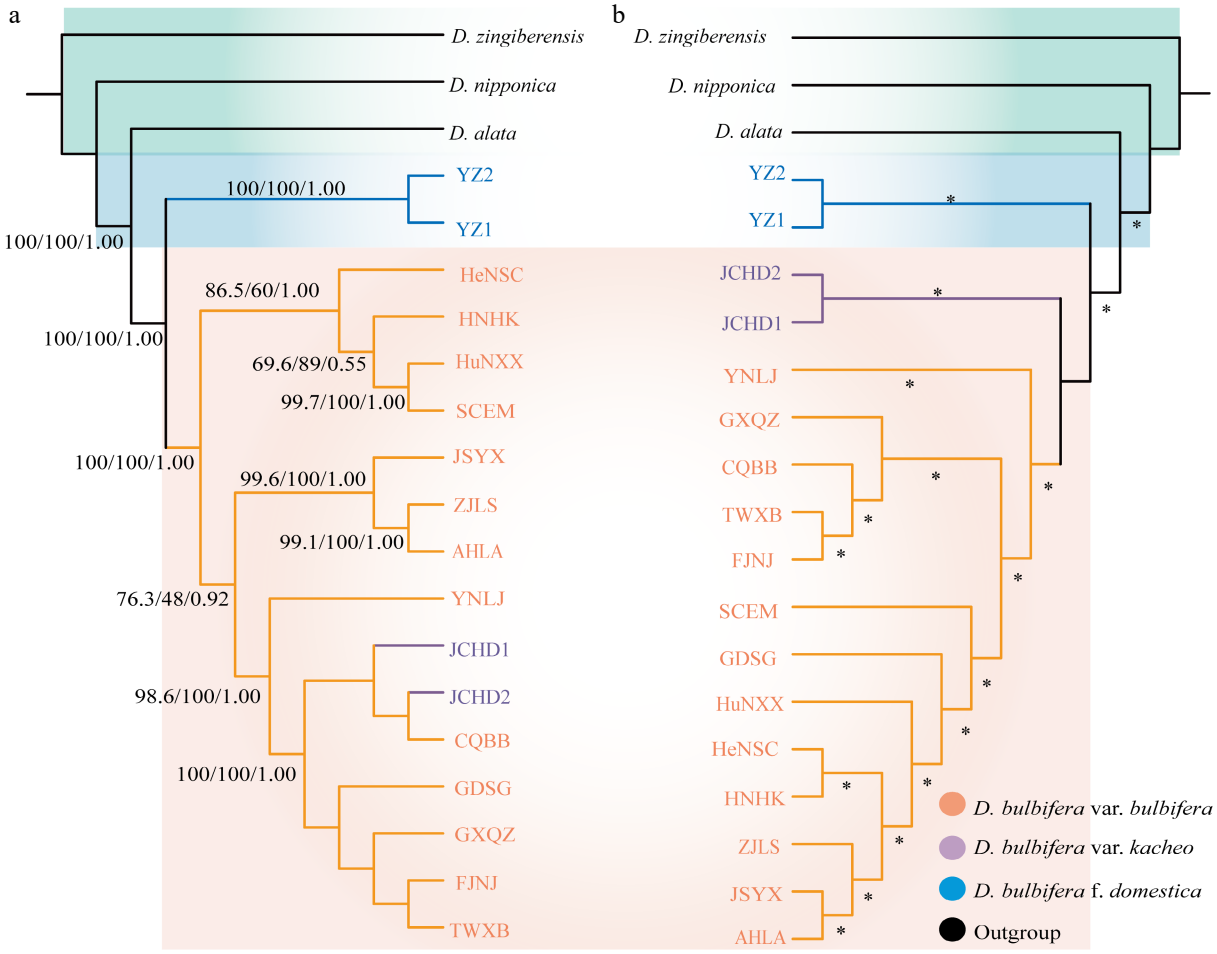


Fig. 5 Phylogenetic relationships and cytonuclear discordance in *D. bulbifera*. (a) Maximum likelihood (ML) tree based on complete plastome sequences; node labels show SH-aLRT/UFBoot/PP (SH-aLRT support [%], ultrafast bootstrap support [%], and Bayesian posterior probabilities). (b) ML tree based on genome-wide nuclear SNPs; node labels show SH-aLRT/UFBoot support (%), with * indicating SH-aLRT/UFBoot = 100/100. All trees were rooted with *D. zingiberensis*.

Cytonuclear discordance and reticulate evolution

The plastome and nuclear SNP trees were concordant in recovering *D. bulbifera* f. *domestica* as a distinct, early-diverging lineage, but they were strongly discordant in the placement of *D. bulbifera* var. *kacheo*. In the plastome phylogeny, the two *D. bulbifera* var. *kacheo* accessions were nested among *D. bulbifera* var. *bulbifera* samples rather than forming a sister lineage to that taxon. In the nuclear SNP tree, by contrast, *D. bulbifera* var. *kacheo* formed an independent, well-supported clade that was sister to all *D. bulbifera* var. *bulbifera* accessions. Plastomes reflect maternal inheritance, whereas nuclear genomes capture biparental evolutionary processes[27]. Cytonuclear discordance is widespread in plants and is typically attributed to incomplete lineage sorting (ILS), hybridization, and introgression[27,56]. These processes may act concurrently, particularly in recently diverged or polyploid lineages.

In this study, population genomic analyses provide complementary evidence for historical gene exchange. Significantly positive *D*-statistics indicate excess allele sharing between *D. bulbifera* var. *kacheo* and *D. bulbifera* f. *domestica* relative to the tested topology[57], and TreeMix recovered a migration edge from *D. bulbifera* f. *domestica* to *D. bulbifera* var. *kacheo*[49]. These results are consistent with introgression contributing to the observed discordance, but they do not exclude a substantial contribution from ILS. Formal discrimination between introgression and retained ancestral polymorphism remains challenging under the multispecies coalescent, especially with limited per-taxon sampling[56,58]. We therefore interpret the phylogenetic incongruence as more consistent with a reticulate evolutionary model than with a strictly bifurcating history, while acknowledging that the relative contributions of introgression and ILS cannot be fully partitioned with the present dataset[56,59]. These patterns are compatible with a reticulate history involving episodic gene flow; given the cytological heterogeneity documented in *D. bulbifera*, interploidy gene flow may also be relevant[18,59,60]. The congruent placement of *D. bulbifera* f. *domestica* in both genomic compartments further indicates that its distinctiveness is not confined to a single inheritance system.

Several limitations should be acknowledged. Only two accessions each of *D. bulbifera* var. *kacheo* and *D. bulbifera* f. *domestica* were available. Consequently, population genetic metrics based on these groups (π, F_{ST}, *D*-statistic, and TreeMix migration weights) should be regarded as exploratory: absolute values may be sensitive to sampling, even though the direction of the patterns was consistent across phylogenies, PCA, ADMIXTURE, differentiation statistics, and gene-flow analyses. For this reason, and consistent with the discussion above, taxonomic conclusions regarding the relative infraspecific rank of *D. bulbifera* var. *kacheo* remain tentative. The clear separation of *D. bulbifera* f. *domestica* across all analyses indicates that its differentiation is unlikely to be solely an artifact of sampling.

https://doi.org/10.48130/tp-0026-0037

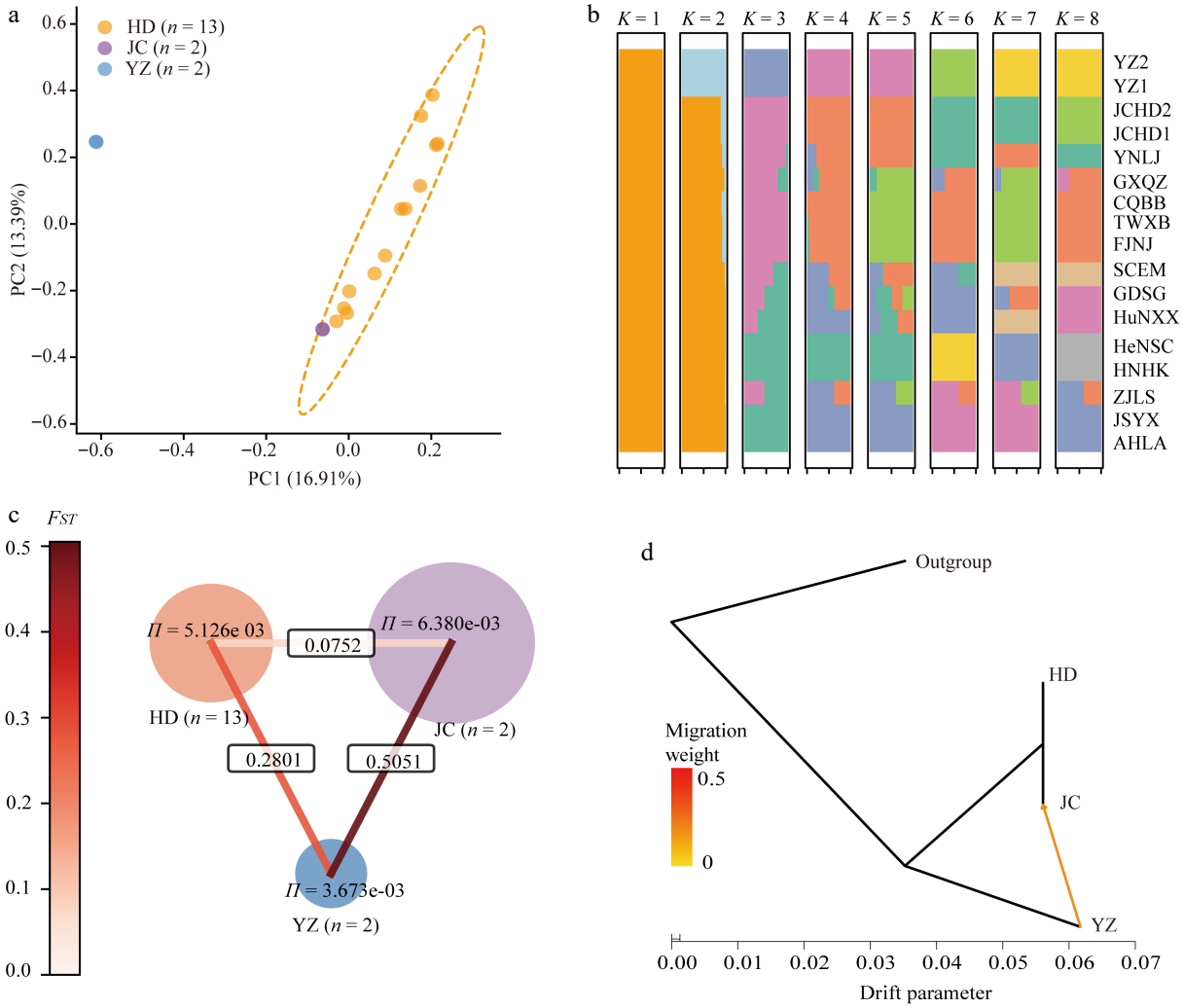


Fig. 6 Population genomic analyses of three *D. bulbifera* infraspecific taxa: HD (*D. bulbifera* var. *bulbifera*), JC (*D. bulbifera* var. *kacheo*), and YZ (*D. bulbifera* f. *domestica*). (a) PCA based on genome-wide SNPs; PC1 and PC2 explain 16.91% and 13.39% of genetic variation. Orange, purple, and blue denote HD (n = 13), JC (n = 2), and YZ (n = 2), respectively. (b) ADMIXTURE analysis (K = 1–8) showing ancestry proportions of each sample. (c) Network of (π) nucleotide diversity and (F_{ST}) population differentiation; values inside circles indicate π, and lines show pairwise F_{ST} (white to red indicates increasing differentiation). (d) TreeMix analysis (m = 1) showing population divergence and gene flow; the yellow arrow indicates migration from YZ to JC (weight = 0.183).

Nevertheless, broader sampling across geographic ranges will be essential for further resolving fine-scale population structure and evaluating the full extent of genetic diversity within each lineage. Future studies integrating larger population datasets and demographic modeling will help to refine the evolutionary history and taxonomic boundaries of *D. bulbifera*.

Conclusions

This study provides an integrative framework for evaluating infraspecific taxonomic relationships within *D. bulbifera* by combining genome-wide nuclear SNP data, plastome variation, cytological evidence, and morphological traits. Our results indicate that *D. bulbifera* f. *domestica* represents a genetically differentiated infraspecific lineage, supported by concordant patterns across phylogenetic and population-genomic analyses. In contrast, *D. bulbifera* var. *kacheo* is morphologically diagnosable but shows only limited genome-wide differentiation from *D. bulbifera* var. *bulbifera*, indicating that phenotypic divergence is not necessarily accompanied by substantial genomic differentiation.

The observed cytonuclear discordance further suggests that the evolutionary history of *D. bulbifera* is unlikely to conform to a strictly bifurcating model. Population-genomic analyses are consistent with historical gene flow contributing to this incongruence; however, incomplete lineage sorting cannot be excluded, and the relative contributions of these processes—and of potential interploidy gene flow—cannot yet be fully partitioned.

Overall, these findings clarify the asymmetric differentiation between historically recognized infraspecific taxa of *D. bulbifera* and underscore the value of integrating morphological, cytological, and genomic evidence when evaluating infraspecific boundaries in taxonomically complex plant groups. Formal nomenclatural revision, however, should await broader geographic sampling.

Author contributions

The authors confirm their contributions to the paper as follows: study conception and design: Zhang YY, Sun XQ, Chen M, Xue JY; material collection: Sun XQ, Chen M; chromosome observation and morphological photograph collection: Chen M; plastome assembly,

phylogenetic analyses, gene flow analyses and drafted the manuscript: Zhang YY; revised and edited the manuscript: Xue JY, Sun XQ, Chen M. All authors reviewed the results and approved the final version of the manuscript.

Data availability

The low-coverage whole-genome sequencing data for 17 *Dioscorea bulbifera* accessions are available in the NCBI SRA database under BioProject PRJNA1442850 (accessions SRR37794138–SRR37794154; see Supplementary Table S3 for details). The plastome assembly and annotation data are available in the CNGB database under project CNP0009382 (accessions CNA0723146–CNA0723162; see Supplementary Table S3 for details).

Acknowledgments

The authors declare financial support was received for the research, authorship, and/or publication of this article. This research was funded by the National Natural Science Foundation of China (32200194 and 32671990).

Conflict of interest

The authors declare that they have no conflict of interest.

Supplementary information accompanies this paper online at: https://doi.org/10.48130/tp-0026-0037.

Dates

Received 24 May 2026; Revised 21 August 2026; Accepted 10 September 2026; Published online 23 October 2026

References

[1] Ding ZZ. 2000. *Dioscorea*. In *Flora of China*, eds. Wu ZY, Raven PH. Vol. 24. Beijing: Science Press; St. Louis: Missouri Botanical Garden Press. pp. 276–296 www.iplant.cn/foc/pdf/Dioscorea.pdf

[2] Kundu BB, Vanni K, Farheen A, Jha P, Pandey DK, et al. 2021. *Dioscorea bulbifera* L. (Dioscoreaceae): a review of its ethnobotany, pharmacology and conservation needs. *South African Journal of Botany* 140:365–374

[3] Sharma S, Kaul S, Dhar MK. 2024. A systematic review on ethnobotany, phytochemistry and pharmacology of *Dioscorea bulbifera* L. (Dioscoreaceae). *South African Journal of Botany* 170:367–393

[4] Zhang Y, Miao J, Zhou D, Xu D, Fu P, et al. 2026. The double-edged sword of *Dioscorea bulbifera* L.: recent advances in its pharmacological benefits and hepatotoxicity, and the quest for detoxification strategies. *Journal of Ethnopharmacology* 362:121331

[5] Makino T. 1912. *Dioscorea sativa* f. *domestica*. In *Somoku-Dzusetsu*, ed. Iinuma Y. 3rd Edition. Tokyo: Seibido. 1326 pp www.huh.harvard.edu/book/somoku-dzusetsu-1907

[6] Makino T, Nemoto K. 1931. *Flora of Japan (Nippon-Shokubutsu-Sōran)*. 2nd Edition. Tokyo: Shunyodo Shoten. 1936 pp http://opac.lib.niigata-u.ac.jp/recordID/catalog.bib/BN01445325

[7] Prain D, Burkill IH. 1914. A synopsis of the *Dioscoreas* of the Old World, Africa excluded, with descriptions of new species and of varieties. *Journal and Proceedings of the Asiatic Society of Bengal* 10:5–41

[8] Knuth R. 1924. *Dioscoreaceae*. In *Das Pflanzenreich: Regni Vegetabilis Conspectus*, ed. Engler A. Leipzig: Wilhelm Engelmann. pp. 88–91 www.biodiversitylibrary.org/bibliography/71249

[9] Prain D, Burkill IH. 1936. *An account of the genus Dioscorea in the East. Part I: The species which twine to the left*. Annals of the Royal Botanic Garden, Calcutta. Alipore: Bengal Government Press. pp. 1–210

[10] Zheng YH, Xia B, Hang YY, Zhou YF, Wang XL, et al. 2006. 黄独遗传多样性分析 [Genetic diversity analysis of *Dioscorea bulbifera*]. *西北植物学报 [Acta Botanica Boreali-Occidentalia Sinica]* 26:2011–2017 (in Chinese)

[11] Zhou YF, Chen M, Sun XQ, Hang YY. 2018. 中国薯蓣科基生翅组的分类修订 [Taxonomic revision of sect. Opsophyton (Dioscoreaceae) in China]. *植物资源与环境学报 [Journal of Plant Resources and Environment]* 27:101–107 (in Chinese)

[12] Hoque A, Lakshminarasimhan P, Maity D. 2018. Lectotypification of thirteen names in *Dioscoreaceae* R.Br. *Pleione* 12:299–308

[13] Noltie HJ. 1994. *Dioscoreaceae*. In *Flora of Bhutan*, ed. Noltie HJ. Edinburgh: Royal Botanic Garden Edinburgh. pp. 9–10 https://hdl.handle.net/20.500.12594/6040

[14] Hamilton CW, Reichard SH. 1992. Current practice in the use of subspecies, variety, and forma in the classification of wild plants. *Taxon* 41:485–498

[15] Lu R, Hu K, Sun X, Chen M. 2024. Low-coverage whole genome sequencing of diverse *Dioscorea bulbifera* accessions for plastome resource development, polymorphic nuclear SSR identification, and phylogenetic analyses. *Frontiers in Plant Science* 15:1373297

[16] Qin HZ, Zhang MZ, Ling PP, Ding ZZ, Dou FP. 1985. 中国薯蓣属细胞分类的研究 — 染色体数与该属起源和演化 [A cytotaxonomic study on Chinese *Dioscorea* L. — The chromosome numbers and their relation to the origin and evolution of the genus]. *植物分类学报 [Acta Phytotaxonomica Sinica]* 23:11–18 (in Chinese)

[17] Gatarira C, Sládeková L, Němečková A, Šimoníková D, Paliwal R, et al. 2021. Cytological and molecular characterization for ploidy determination in yams (*Dioscorea* spp.). *Agronomy* 11:1897

[18] Brown MR, Abbott RJ, Twyford AD. 2024. The emerging importance of cross-ploidy hybridisation and introgression. *Molecular Ecology* 33:e17315

[19] Martin FW, Ortiz S. 1963. Chromosome numbers and behavior in some species of *Dioscorea*. *Cytologia* 28:96–101

[20] Sugihara Y, Darkwa K, Yaegashi H, Natsume S, Shimizu M, et al. 2020. Genome analyses reveal the hybrid origin of the staple crop white Guinea yam (*Dioscorea rotundata*). *Proceedings of the National Academy of Sciences of the United States of America* 117:31987–31992

[21] Scarcelli N, Cubry P, Akakpo R, Thuillet AC, Obidiegwu J, et al. 2019. Yam genomics supports West Africa as a major cradle of crop domestication. *Science Advances* 5:eaaw1947

[22] Adjei EA, Esuma W, Alicai T, Bhattacharjee R, Dramadri IO, et al. 2023. Genetic diversity and population structure of Uganda's yam (*Dioscorea* spp.) genetic resource based on DArTseq. *PLoS One* 18:e0277537

[23] Cormier F, Lawac F, Maledon E, Gravillon MC, Nudol E, et al. 2019. A reference high-density genetic map of greater yam (*Dioscorea alata* L.). *Theoretical and Applied Genetics* 132:1733–1744

[24] Feng W, Zhang Z, Zhang J, Nan P, Song Z, et al. 2024. Comparative plastomic analysis of cultivated *Dioscorea polystachya* and its close relatives provides insights on the inter- and intraspecific phylogenies and potential wild origins of domestication. *BMC Plant Biology* 24:1255

[25] Ekaette E, Nwofia E, Okocha P, Nnnabue I, Eluwa K, et al. 2024. Exploring the genetic diversity and population structure of aerial yams (*Dioscorea bulbifera* L.) DArT-seq and agronomic traits. *PLoS One* 19:e0306631

[26] Silva DM, Siqueira MVBM, Carrasco NF, Mantello CC, Nascimento WF, et al. 2016. Genetic diversity among air yam (*Dioscorea bulbifera*) varieties based on single sequence repeat markers. *Genetics and Molecular Research* 15:gmr.15027929

[27] Duan L, Fu L, Chen HF. 2023. Phylogenomic cytonuclear discordance and evolutionary histories of plants and animals. *Science China Life Sciences* 66:2946–2948

[28] Babil PK, Kikuno H, Shiwachi H, Toyohara H, Fujigaki J, et al. 2010. Optimum Time for Collection of Root Samples for Chromosome Observation in Yams (*Dioscorea* spp.). *Tropical Agriculture and Development* 54:71–75

[29] Sliwinska E, Loureiro J, Leitch IJ, Šmarda P, Bainard J, et al. 2022. Application-based guidelines for best practices in plant flow cytometry. *Cytometry Part A* 101:749–781

https://doi.org/10.48130/tp-0026-0037

[30] Loureiro J, Rodriguez E, Doležel J, Santos C. 2007. Two new nuclear isolation buffers for plant DNA flow cytometry: a test with 37 species. *Annals of Botany* 100:875–888
[31] Chen S, Zhou Y, Chen Y, Gu J. 2018. fastp: an ultra-fast all-in-one FASTQ preprocessor. *Bioinformatics* 34:i884–i890
[32] Jin JJ, Yu WB, Yang JB, Song Y, dePamphilis CW, et al. 2020. GetOrganelle: a fast and versatile toolkit for accurate de novo assembly of organelle genomes. *Genome Biology* 21:241
[33] Tillich M, Lehwark P, Pellizzer T, Ulbricht-Jones ES, Fischer A, et al. 2017. GeSeq – versatile and accurate annotation of organelle genomes. *Nucleic Acids Research* 45:W6–W11
[34] Amiryousefi A, Hyvönen J, Poczai P. 2018. IRscope: an online program to visualize the junction sites of chloroplast genomes. *Bioinformatics* 34:3030–3031
[35] Katoh K, Standley DM. 2013. MAFFT multiple sequence alignment software version 7: improvements in performance and usability. *Molecular Biology and Evolution* 30:772–780
[36] Capella-Gutiérrez S, Silla-Martínez JM, Gabaldón T. 2009. trimAl: a tool for automated alignment trimming in large-scale phylogenetic analyses. *Bioinformatics* 25:1972–1973
[37] Minh BQ, Schmidt HA, Chernomor O, Schrempf D, Woodhams MD, et al. 2020. IQ-TREE 2: new models and efficient methods for phylogenetic inference in the genomic era. *Molecular Biology and Evolution* 37:1530–1534
[38] Kalyaanamoorthy S, Minh BQ, Wong TKF, von Haeseler A, Jermiin LS. 2017. ModelFinder: fast model selection for accurate phylogenetic estimates. *Nature Methods* 14:587–589
[39] Ronquist F, Teslenko M, van der Mark P, Ayres DL, Darling A, et al. 2012. MrBayes 3.2: efficient Bayesian phylogenetic inference and model choice across a large model space. *Systematic Biology* 61:539–542
[40] Rambaut A, Drummond AJ, Xie D, Baele G, Suchard MA. 2018. Posterior summarization in Bayesian phylogenetics using tracer 1.7. *Systematic Biology* 67:901–904
[41] Rocher S, Jean M, Castonguay Y, Belzile F. 2015. Validation of genotyping-by-sequencing analysis in populations of tetraploid alfalfa by 454 sequencing. *PLoS One* 10:e0131918
[42] de C Lara LA, Santos MF, Jank L, Chiari L, de M Vilela M, et al. 2019. Genomic selection with allele dosage in *Panicum maximum* jacq. *G3: Genes | Genomes | Genetics* 9:2463–2475
[43] Kendig KI, Baheti S, Bockol MA, Drucker TM, Hart SN, et al. 2019. Sentieon DNASeq variant calling workflow demonstrates strong computational performance and accuracy. *Frontiers in Genetics* 10:736
[44] Van der Auwera GA, Carneiro MO, Hartl C, Poplin R, Del Angel G, et al. 2013. From FastQ data to high confidence variant calls: the Genome Analysis Toolkit best practices pipeline. *Current Protocols in Bioinformatics* 43:11.10.1–11.10.33
[45] Chang CC, Chow CC, Tellier LC, Vattikuti S, Purcell SM, et al. 2015. Second-generation PLINK: rising to the challenge of larger and richer datasets. *GigaScience* 4:7
[46] Bradbury PJ, Zhang Z, Kroon DE, Casstevens TM, Ramdoss Y, et al. 2007. TASSEL: software for association mapping of complex traits in diverse samples. *Bioinformatics* 23:2633–2635
[47] Danecek P, Auton A, Abecasis G, Albers CA, Banks E, et al. 2011. The variant call format and VCFtools. *Bioinformatics* 27:2156–2158
[48] Malinsky M, Matschiner M, Svardal H. 2021. Dsuite - Fast *D*-statistics and related admixture evidence from VCF files. *Molecular Ecology Resources* 21:584–595
[49] Pickrell JK, Pritchard JK. 2012. Inference of population splits and mixtures from genome-wide allele frequency data. *PLoS Genetics* 8:e1002967
[50] Fitak RR. 2021. *OptM*: estimating the optimal number of migration edges on population trees using *Treemix*. *Biology Methods & Protocols* 6:bpab017
[51] Alexander DH, Novembre J, Lange K. 2009. Fast model-based estimation of ancestry in unrelated individuals. *Genome Research* 19:1655–1664
[52] De Queiroz K. 2007. Species concepts and species delimitation. *Systematic Biology* 56:879–886
[53] Campos M, Kelley E, Gravendeel B, Médail F, Maarten Christenhusz JM, et al. 2023. Genomic, spatial and morphometric data for discrimination of four species in the Mediterranean Tamus clade of yams (*Dioscorea*, Dioscoreaceae). *Annals of Botany* 131:635–654
[54] Franzoni J, Astuti G, Peruzzi L. 2023. Weak genetic isolation and putative phenotypic selection in the wild carnation *Dianthus virgineus* (Caryophyllaceae). *Biology* 12:1355
[55] Zhang W, Wang H, Zhang T, Fang X, Liu M, et al. 2023. Geographic–genomic and geographic–phenotypic differentiation of the *Aquilegia viridiflora* complex. *Horticulture Research* 10:uhad041
[56] Degnan JH, Rosenberg NA. 2009. Gene tree discordance, phylogenetic inference and the multispecies coalescent. *Trends in Ecology & Evolution* 24:332–340
[57] Durand EY, Patterson N, Reich D, Slatkin M. 2011. Testing for ancient admixture between closely related populations. *Molecular Biology and Evolution* 28:2239–2252
[58] Hibbins MS, Hahn MW. 2022. Phylogenomic approaches to detecting and characterizing introgression. *Genetics* 220:iyab173
[59] Stull GW, Pham KK, Soltis PS, Soltis DE. 2023. Deep reticulation: the long legacy of hybridization in vascular plant evolution. *The Plant Journal* 114:743–766
[60] Bartolić P, Morgan EJ, Padilla-García N, Kolář F. 2024. Ploidy as a leaky reproductive barrier: mechanisms, rates and evolutionary significance of interploidy gene flow. *Annals of Botany* 134:537–550

Copyright: © 2026 by the author(s). Published by Maximum Academic Press on behalf of Hainan University. This article is an open access article distributed under Creative Commons Attribution License (CC BY 4.0), visit https://creativecommons.org/licenses/by/4.0/.